Transients in water systems generated by air release valves

G. De Martino, N. Fontana**, M. Giugni**
** Dip. di Ing. Idraulica ed Ambientale "G. Ippolito", Università di Napoli Federico II*
*** Dipartimento di Ingegneria, Università del Sannio*

1 ABSTRACT

The presence of air in pressurised water systems may frequently give rise to not negligible problems occurring both during normal operating conditions and when the system is being filled, for example following maintenance interventions. This paper presents the results of a wide-ranging experimental investigation to examine pressure surges generated by the venting of air pockets from a pressurised pipe ending in an automatic release valve. A detailed picture of the test results is presented, the characteristics of the hydraulic surges recorded are shown, and a mathematical model allowing an acceptable simulation of pressure surges is discussed.

2 INTRODUCTION

The presence of air in pressurised water systems may give rise to serious operating problems, such as a decrease in system transport capacity or the rise of pressure surges caused by the reduction of the flow section (1). The use of mechanical air release valves suitably located along pipelines provides adequate venting and ensures that air pockets, and the resulting problems, do not arise.

However, the functioning of air valves may trigger pressure surges, sometimes of unexpected magnitude (2), (3), (4). Despite numerous significant contributions (5), (6), (7), (8), (9), (10), (11), (12), analysis of the above pressure surges does not seem to have reached a satisfactory stage (13), (14).

In order to further clarify these issues, it is thus of considerable interest - in the wake of experiments already conducted by other authors (15) and by the writers (16) - to examine pressure surges following the venting of air pockets from a pressurised pipe ending in a commercial air release valve.

In the present paper, the results of the experiments carried out are reported, the characteristics of the recorded pressure transients are examined, and a mathematical model allowing an acceptable simulation of pressure surges is discussed.

3 EXPERIMENTAL SET-UP

The experimental apparatus set up in the Laboratory of the Dipartimento di Ingegneria Idraulica ed Ambientale *G. Ippolito* at the University of Naples *Federico II*, is comprised of

(Figure 1) a galvanised iron pipe measuring 2” (53 mm) in diameter and 69.62 m in length, departing from a steel ∅ 300 mm pipe from the Laboratory’s main circuit via a pipe section fitted with a ball valve which pressurises the experimental pipe when opened.

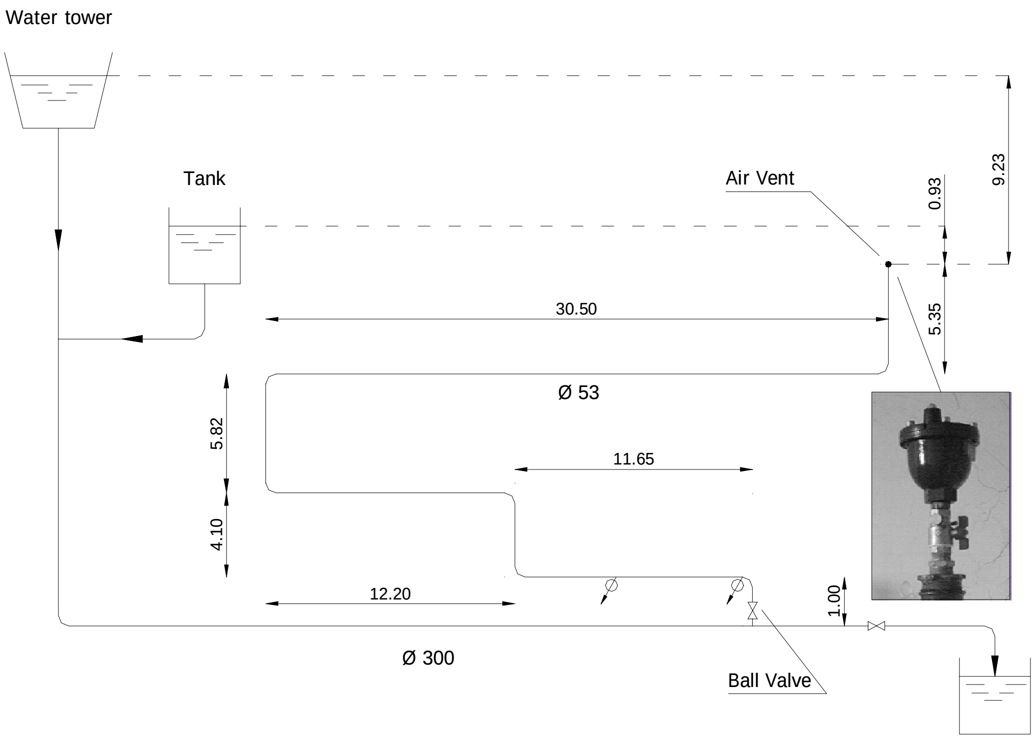

Figure 1. Scheme of experimental set-up.

On the end of the pipe was installed a ball valve followed by a commercial automatic air release valve (single chamber with a stainless steel spherical float operated by a compass compound lever) (Figure 2).

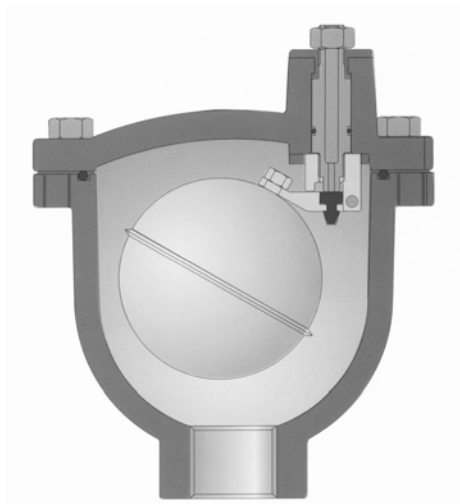

Figure 2. Scheme of mechanical air vent.

The tests required the pressurised pipe to be vented by opening the ball valve and measuring the pressure surge during air release until the release valve closed. Other tests were carried out closing the end of the vertical section with a ball valve and a simple cap containing a centred, sharp-edged orifice.

The pressure was measured using a WIKA™ pressure transducer mod. 891.13.520, installed immediately upstream of the ball valve and set for a 0÷10 bar measurement interval and with a current output signal varying in the range 4÷20 mA. Signal acquisition was achieved using a National Instruments™ AT-MIO-16E-10 analogue-digital converter, running a LabView™ application for Windows™, and at an acquisition frequency of 250 Hz, in view of the characteristics of the pressure surges to be recorded.

The experiments were carried out while varying the pressure head on the orifice H_0, the air pocket volume measured with respect to the length of the air column Z_0, and the diameter d of the nozzle of the mechanical release valve (or of the orifice). In particular:

- H_0 = 9.23 m (hydraulic circuit supplied by the water tower; Figure 1)
  = 0.93 m (hydraulic circuit supplied by the tank; Figure 1)
- Z_0 = 0.30 m; 0.50 m; 0.70 m; 1.00 m
- d = 1.2 mm; 1.4 mm; 1.8 mm

Each test was repeated several times (at least 5 times) to check for the presence of any random phenomena during the pressure surge.

4 EXPERIMENTAL TESTS

As mentioned above, the experiments were carried out in order to measure the pressure transient p(t) from the opening of the ball valve immediately upstream of the valve to the closure of the device (or after the liquid column had impacted on the orifice).

The experiments carried out on the orifices gave rise to a hydraulic transient consisting of two phases, as already pointed out by various authors (2), (10), (11) and as can be seen in the trend of p(t) reported as an example in Figure 3 (H_0=9.23 m, Z_0=1 m, d=1.8 mm):

- an initial phase of rigid column motion arising as soon as the ball valve was opened, with the release of air from the orifice;
- a second water hammer phase as the water impacts on the orifice. In particular, this phase is initially characterised by a sudden increase in pressure (impact phase) due of course to the sudden deceleration of the liquid column because of the considerable difference in density between air and water (2), (5), (6). This phase has already been examined with reference to the simple venting and the filling of a pipe, both by the present writers and by other authors (7), (8), (10), (11), (14), (17). The impact phase has an evident slope variation in the trend of the pressure curve, followed by a sudden increase in pressure up to a maximum value, p_{max}. It is also characterised by oscillations around p_{max} (Figure 3). Thereafter, the pressure surges caused by the impact tend to become progressively dampened as a result of the head losses.

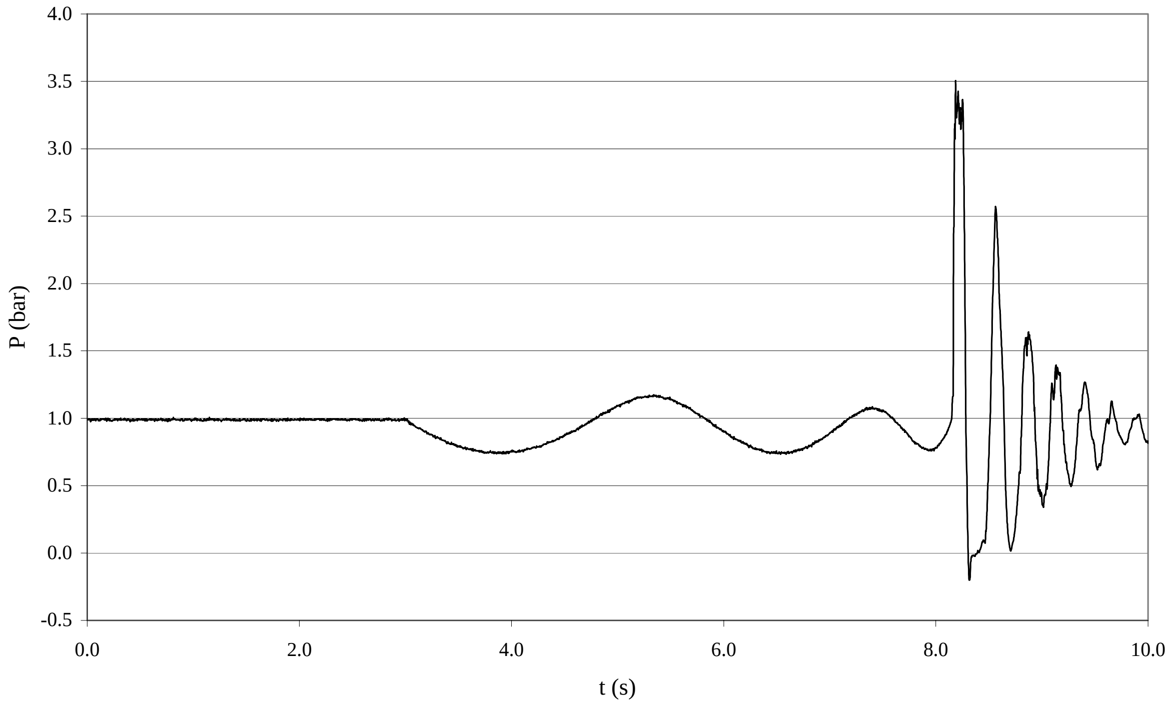

Figure 3. Pressure surge following release of air from an orifice.

The experiments carried out with the orifice substituted by a commercial release valve yielded qualitatively similar hydraulic transients characterised by some clear differences in the trend of p(t) with respect to the previous measurements, as can be seen in the plots reported as an example in Figure 4 (H_0=9.23 m, Z_0=1 m, d=1.8 mm) and Figure 5 (H_0=0.93 m, Z_0=1.00 m, d=1.8 mm).

In order to make them easier to interpret, the transients are schematised in three phases:

- Phase I: the almost instantaneous opening of the ball valve coincides with the sudden drop in pressure (sub-vertical section in Figures 4 and 5);
- Phase II (venting): the outflow of air from the release valve until the float blocks the nozzle creates the classic rigid column pressure transient typical of the venting phase;
- Phase III: the start of phase III is characterised by a clear cusp in the trend of p(t) (cfr. Figures 4 and 5), followed by a rapid increase in pressure up to the maximum value, which is, however, characterised by a clear peak. As already recently pointed out by the writers (16), this trend is quite different from the one observed by substituting a simple orifice for a commercial valve: in this case the mass oscillations phase is followed by a water hammer determined by the water column impacting on the orifice following the venting operation and characterised by significantly lower period values and higher surge values (Figure 3).

For each of the experiments carried out, the following measurements were taken:

- initial partial decompression of the air column (ΔH_1);
- duration (T) of the transient's second phase (venting);
- maximum negative (ΔH_2) and positive (ΔH_3) pressure variation in the second phase, with reference to the pressure value at the start of the test;
- maximum positive (ΔH_4) and negative (ΔH_5) pressure variation in the third phase of

the transient, with reference to the pressure value at the start of the test.

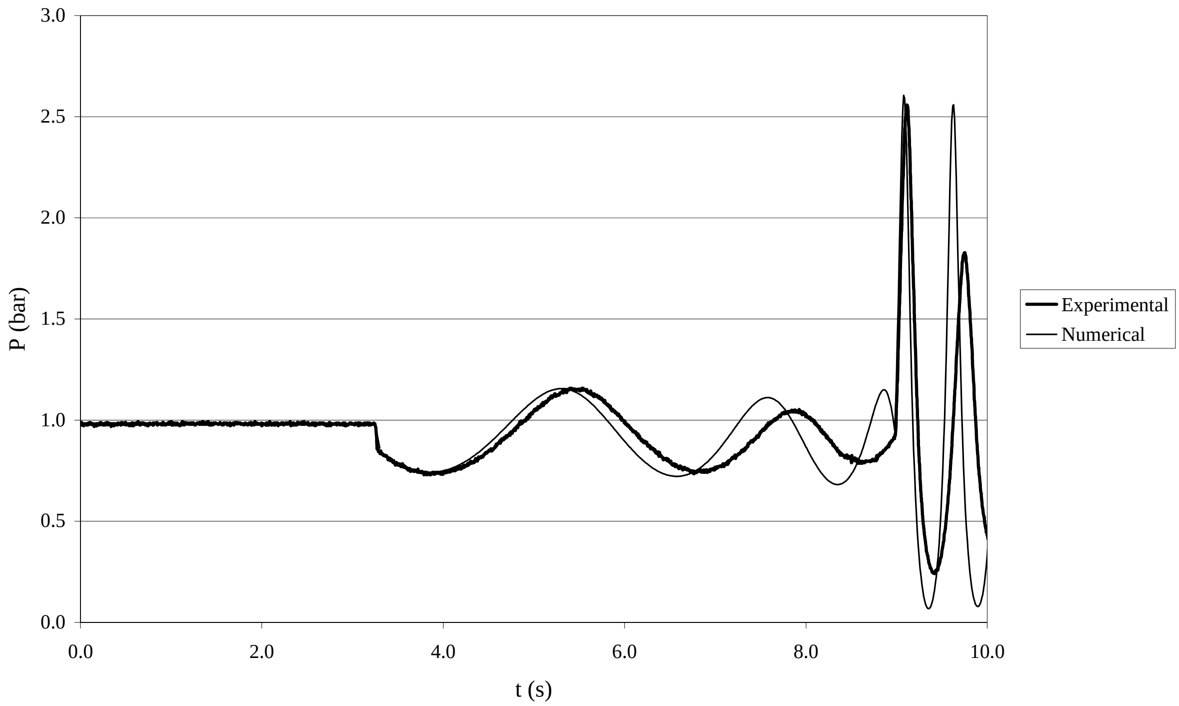

Figure 4. Pressure surge following release of air from an air release valve (H_0=9.23 m).

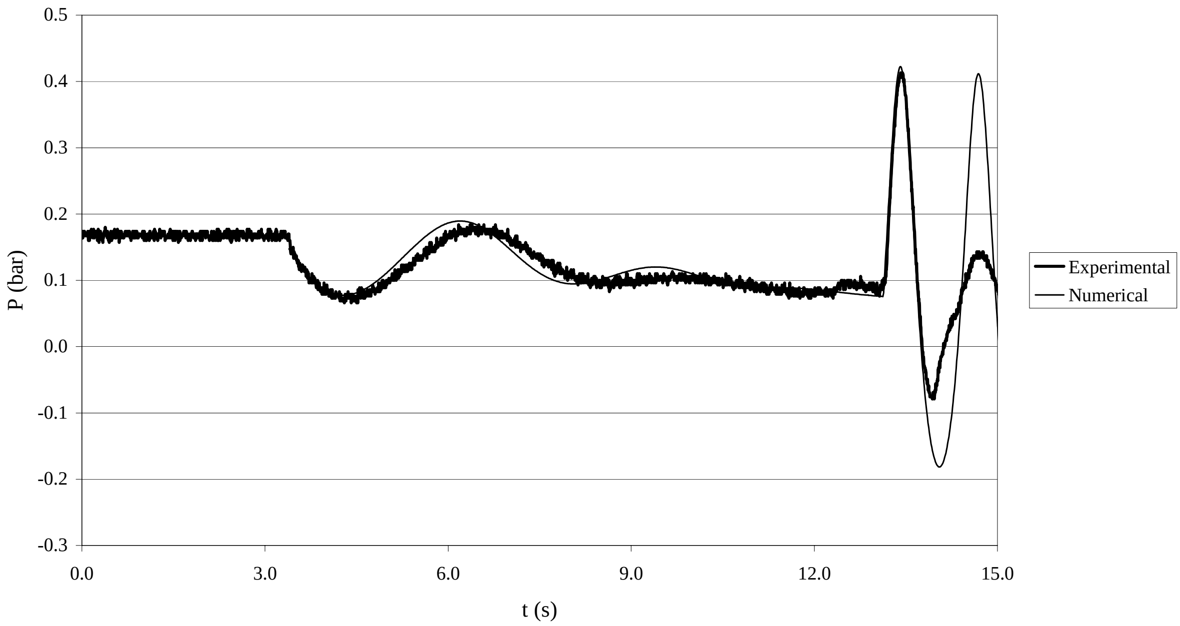

Figure 5. Pressure surge following release of air from an air release valve (H_0=0.93 m).

The values of the above parameters are reported in Tables 1-6, together with the tests' order number and the values of H_0, Z_0 and d.

Order Number	Z_0 (m)	ΔH_1 (m)	ΔH_2 (m)	ΔH_3 (m)	T (s)	ΔH_4 (m)	ΔH_5 (m)
1	0.30	-3.084	-3.767	4.265	7.445	4.469	-3.217
2	0.30	-3.090	-3.844	4.086	8.046	4.402	-3.192
3	0.30	-3.265	-3.846	4.125	8.650	4.461	-3.163
4	0.30	-2.890	-3.848	4.082	7.818	4.500	-3.124
5	0.30	-2.818	-3.847	4.052	8.262	4.429	-3.124
6	0.50	-1.940	-2.837	2.657	9.550	7.539	-4.794
7	0.50	-2.157	-2.809	2.654	12.062	7.537	-4.838
8	0.50	-2.188	-2.871	2.654	10.142	7.567	-4.838
9	0.50	-2.295	-2.846	2.648	10.574	7.561	-4.803
10	0.50	-2.162	-2.875	2.649	9.938	7.491	-4.802
11	0.70	-1.739	-2.360	1.941	11.326	6.711	-4.827
12	0.70	-1.706	-2.389	1.943	11.518	6.642	-4.825
13	0.70	-1.735	-2.356	1.904	11.478	6.746	-4.864
14	0.70	-1.768	-2.359	1.901	11.322	6.610	-4.826
15	0.70	-1.736	-2.317	1.944	11.458	6.847	-4.896
16	1.00	-1.249	-1.861	1.431	14.343	6.039	-5.062
17	1.00	-1.316	-1.907	1.426	14.843	5.788	-4.853
18	1.00	-1.211	-1.904	1.327	14.335	5.557	-4.748
19	1.00	-1.212	-1.936	1.367	14.495	5.587	-4.820
20	1.00	-1.316	-1.907	1.365	14.251	5.686	-4.853

Table 1. Experimental tests (H_0=9.23 m, d=1.2 mm).

Order Number	Z_0 (m)	ΔH_1 (m)	ΔH_2 (m)	ΔH_3 (m)	T (s)	ΔH_4 (m)	ΔH_5 (m)
1	0.30	-3.292	-4.087	4.230	5.729	7.492	-4.566
2	0.30	-3.221	-4.047	4.159	5.689	8.521	-4.974
3	0.30	-3.262	-4.047	4.230	5.681	8.623	-4.944
4	0.30	-3.262	-4.047	4.159	5.877	7.421	-4.597
5	0.30	-3.262	-4.047	4.261	5.733	7.971	-4.801
6	0.50	-2.253	-3.007	2.762	7.409	10.285	-5.759
7	0.50	-2.181	-3.038	2.660	6.921	10.213	-5.759
8	0.50	-2.151	-3.007	2.691	7.197	10.183	-5.718
9	0.50	-2.253	-3.007	2.660	7.714	9.979	-5.616
10	0.50	-2.212	-3.038	2.691	7.197	10.285	-5.820
11	0.70	-1.753	-2.518	2.018	8.574	6.931	-4.638
12	0.70	-1.702	-2.528	2.008	8.582	6.992	-4.648
13	0.70	-1.753	-2.518	2.018	9.522	6.901	-4.607
14	0.70	-1.763	-2.487	2.008	8.982	7.064	-4.648
15	0.70	-1.651	-2.477	2.018	8.754	6.799	-4.536
16	1.00	-1.295	-2.090	1.519	12.122	7.461	-5.321
17	1.00	-1.274	-2.059	1.509	11.490	7.421	-5.331
18	1.00	-1.305	-2.059	1.539	11.526	7.482	-5.433
19	1.00	-1.264	-2.018	1.488	12.030	7.461	-5.382
20	1.00	-1.295	-2.049	1.488	11.798	7.288	-5.351

Table 2. Experimental tests (H_0=9.23 m, d=1.4 mm).

Order Number	Z_0 (m)	ΔH_1 (m)	ΔH_2 (m)	ΔH_3 (m)	T (s)	ΔH_4 (m)	ΔH_5 (m)
1	0.30	-3.619	-4.689	5.311	5.009	10.835	-5.779
2	0.30	-3.619	-4.689	5.239	5.145	11.905	-6.055
3	0.30	-3.445	-4.719	5.209	4.885	11.426	-5.851
4	0.30	-3.313	-4.719	5.209	4.665	11.426	-5.922
5	0.30	-3.486	-4.689	5.209	5.033	11.528	-5.953
6	0.30	-3.353	-4.689	5.514	5.073	9.051	-5.311
7	0.30	-3.282	-4.719	5.474	5.157	8.124	-4.862
8	0.30	-3.384	-4.689	5.514	4.041	7.818	-4.831
9	0.30	-3.353	-4.617	5.514	4.981	8.848	-5.209
10	0.30	-3.292	-4.597	5.504	5.133	9.724	-5.555
11	0.30	-3.353	-4.689	5.616	5.093	8.766	-5.168
12	0.30	-3.282	-4.658	5.514	4.893	9.021	-5.239
13	0.30	-3.394	-4.668	5.463	4.977	9.113	-5.280
14	0.30	-3.313	-4.658	5.514	5.209	8.572	-5.097
15	0.30	-3.394	-4.668	5.535	5.037	8.593	-5.107
16	0.50	-2.232	-3.639	3.262	5.961	7.971	-4.740
17	0.50	-2.273	-3.680	3.231	6.069	6.829	-3.955
18	0.50	-2.232	-3.608	3.364	6.273	15.351	-6.595
19	0.50	-2.202	-3.608	3.394	6.169	15.595	-6.636
20	0.50	-2.202	-3.680	3.435	6.009	9.724	-5.188

Table 3. Experimental tests (H_0=9.23 m, d=1.8 mm).

Order Number	Z_0 (m)	ΔH_1 (m)	ΔH_2 (m)	ΔH_3 (m)	T (s)	ΔH_4 (m)	ΔH_5 (m)
1	0.30	-0.326	-0.775	0.255	10.214	1.417	-0.917
2	0.30	-0.438	-0.775	0.214	11.230	1.315	-0.917
3	0.30	-0.367	-0.815	0.214	10.570	1.315	-0.948
4	0.30	-0.438	-0.775	0.183	10.542	1.315	-0.877
5	0.30	-0.469	-0.815	0.255	10.386	1.315	-0.917
6	0.50	-0.245	-0.764	0.234	14.202	1.091	-1.142
7	0.50	-0.285	-0.764	0.265	14.514	1.162	-1.111
8	0.50	-0.357	-0.764	0.265	16.607	1.162	-1.111
9	0.50	-0.296	-0.775	0.224	16.743	1.111	-1.152
10	0.50	-0.296	-0.744	0.255	13.854	1.111	-1.152
11	0.70	-0.316	-0.764	0.265	16.987	0.958	-1.345
12	0.70	-0.255	-0.775	0.255	17.483	0.948	-1.284
13	0.70	-0.245	-0.724	0.265	17.287	0.958	-1.315
14	0.70	-0.347	-0.764	0.306	17.491	0.989	-1.345
15	070	-0.316	-0.764	0.265	17.375	0.989	-1.315
16	1.00	-0.173	-0.999	0.234	20.639	0.581	-1.651
17	1.00	-0.245	-0.999	0.234	21.199	0.581	-1.621
18	1.00	-0.245	-0.999	0.234	21.527	0.612	-1.621
19	1.00	-0.071	-0.856	0.377	21.563	0.754	-1.478
20	1.00	-0.275	-1.029	0.306	17.603	0.581	-1.621

Table 4. Experimental tests (H_0=0.93 m, d=1.2 mm).

Order Number	Z_0 (m)	ΔH_1 (m)	ΔH_2 (m)	ΔH_3 (m)	T (s)	ΔH_4 (m)	ΔH_5 (m)
1	0.30	-0.379	-0.817	0.171	8.398	1.517	-1.032
2	0.30	-0.483	-0.820	0.169	8.086	1.586	-1.034
3	0.30	-0.346	-0.825	0.134	8.430	1.510	-1.069
4	0.30	-0.384	-0.823	0.207	8.238	1.542	-1.037
5	0.30	-0.407	-0.784	0.174	8.054	1.520	-1.028
6	0.50	-0.265	-0.815	0.214	10.698	1.244	-1.193
7	0.50	-0.347	-0.826	0.234	10.574	1.376	-1.203
8	0.50	-0.245	-0.826	0.234	10.694	1.305	-1.203
9	0.50	-0.336	-0.815	0.245	10.650	1.345	-1.264
10	0.50	-0.336	-0.856	0.245	10.670	1.244	-1.233
11	0.70	-0.265	-0.846	0.214	13.350	1.040	-1.437
12	0.70	-0.234	-0.846	0.255	13.250	1.111	-1.396
13	0.70	-0.265	-0.815	0.285	13.218	1.142	-1.437
14	0.70	-0.234	-0.846	0.255	13.186	1.111	-1.437
15	0.70	-0.234	-0.815	0.285	13.438	1.111	-1.437
16	1.00	-0.255	-1.009	0.265	17.102	0.846	-1.733
17	1.00	-0.214	-0.968	0.265	17.014	0.846	-1.733
18	1.00	-0.255	-0.968	0.265	16.958	0.815	-1.692
19	1.00	-0.224	-0.979	0.285	17.190	0.877	-1.774
20	1.00	-0.255	-0.968	0.265	17.262	0.775	-1.692

Table 5. Experimental tests (H_0=0.93 m, d=1.4 mm).

Order Number	Z_0 (m)	ΔH_1 (m)	ΔH_2 (m)	ΔH_3 (m)	T (s)	ΔH_4 (m)	ΔH_5 (m)
1	0.30	-0.408	-0.917	0.071	7.097	3.404	-1.957
2	0.30	-0.507	-0.914	0.074	6.985	3.275	-1.883
3	0.30	-0.441	-0.890	0.140	7.145	3.330	-1.889
4	0.30	-0.374	-0.986	0.044	7.201	3.336	-1.883
5	0.30	-0.378	-0.959	0.172	7.197	3.332	-1.917
6	0.50	-0.306	-0.989	0.143	8.882	3.099	-2.090
7	0.50	-0.306	-0.989	0.112	8.846	3.170	-2.090
8	0.50	-0.265	-0.989	0.112	8.706	3.099	-2.090
9	0.50	-0.306	-0.989	0.112	8.842	3.170	-2.090
10	0.50	-0.408	-0.989	0.143	8.786	3.129	-2.018
11	0.70	-0.326	-1.009	0.194	10.102	2.905	-2.283
12	0.70	-0.357	-1.009	0.153	10.210	2.905	-2.314
13	0.70	-0.265	-1.019	0.183	10.194	2.864	-2.222
14	0.70	-0.357	-1.009	0.153	10.058	2.936	-2.242
15	0.70	-0.296	-1.060	0.143	10.174	2.895	-2.293
16	1.00	-0.285	-1.040	0.163	13.162	2.497	-2.518
17	1.00	-0.316	-1.040	0.194	12.890	2.569	-2.518
18	1.00	-0.275	-1.070	0.204	12.882	2.579	-2.538
19	1.00	-0.245	-1.029	0.204	12.970	2.609	-2.609
20	1.00	-0.285	-1.040	0.163	12.666	2.630	-2.548

Table 6. Experimental tests (H_0=0.93 m, d=1.8 mm).

Figures 6 and 7 also report the maximum pressure surge values ΔH_4 (of greater interest from

the technical standpoint) as a function of air pocket length Z_0, as the orifice diameter d and the static pressure H_0 vary (equal to 9.23 m in Figure 6 and 0.93 m in Figure 7).
An examination of the experimental data allowed the following observations to be made:

- repeated tests, with the same values of H_0, Z_0 and d, showed deviations of a certain magnitude during the third phase of the transient, particularly for the ΔH_4 value;
- the ΔH_4 values clearly depend on the static pressure: for the same values of d and Z_0, in the tests with the system supplied by the water tower, significantly higher pressure surge values were measured (Figures 6 and 7);
- the magnitude of the pressure surge in the transient's third phase is also significantly affected by d. There is a clear increase in the values of ΔH_4 measured as the nozzle diameter increases;
- whereas the air pocket volume appears to be of little significance as, for the same values of H_0 and d, it does not give rise to significant variations in surge pressure;
- overall, the magnitude of the measured surge pressures seems fairly small: in fact, for H_0=9.23 m, the values of ΔH_4 are always lower than 17 m (Figure 6), while for H_0=0.93 m the highest surge pressures (for d=1.8 mm) are nearly 3.5 m (Figure 6). Note that, in this respect, similar venting tests carried out with a simple orifice instead of the release valve allowed much higher surge pressures to be measured, in the order of 27 m for H_0=9.23 m and 12 m for H_0=0.93 m.

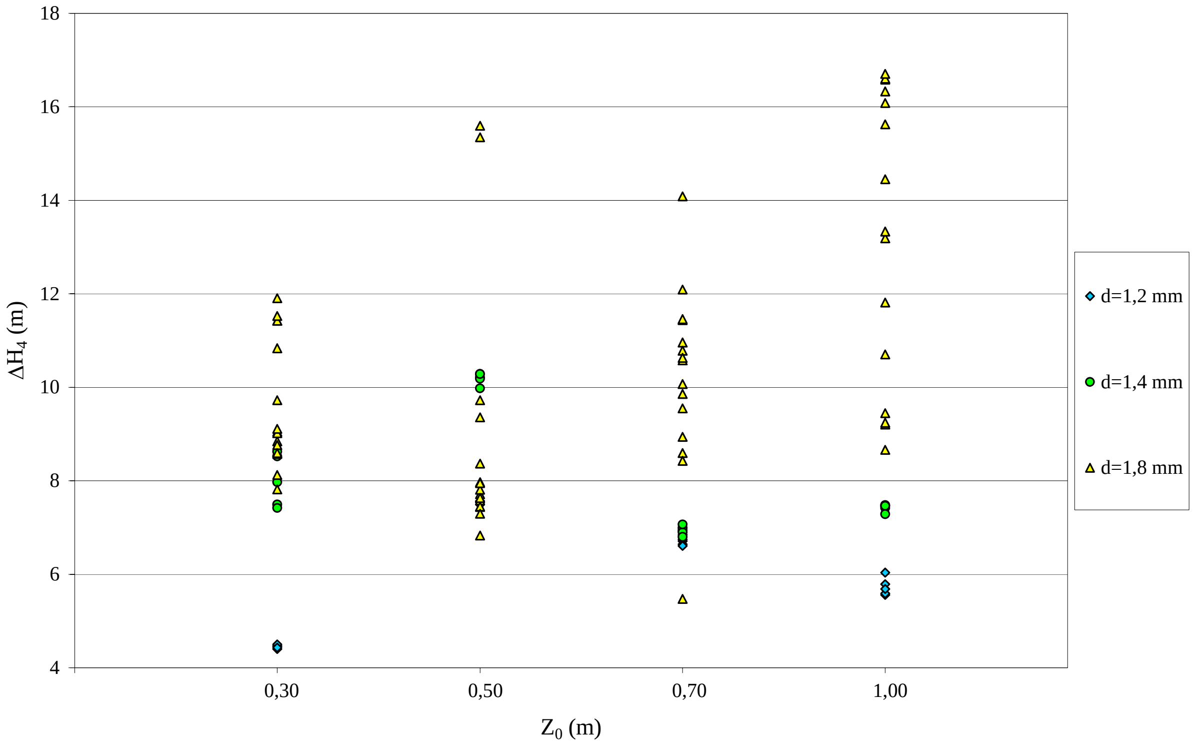

Figure 6. Maximum pressure surge values versus air pocket length (H_0=9.23 m).

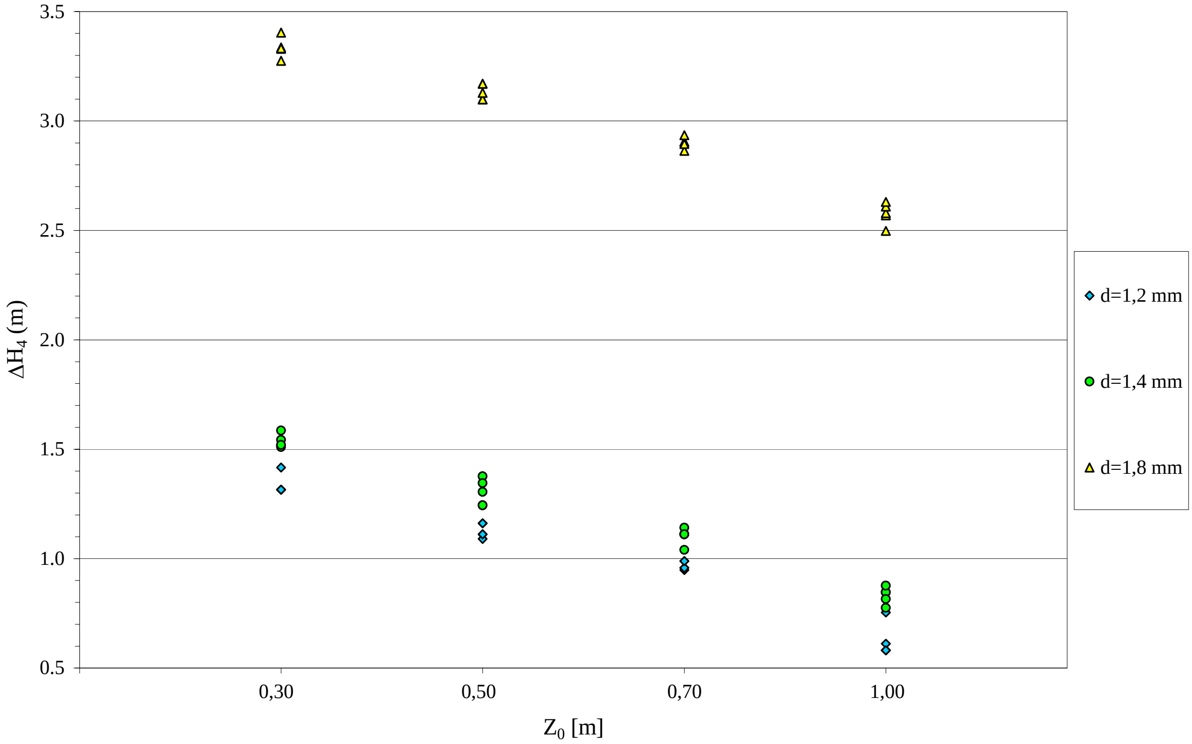

Figure 7. Maximum pressure surge values versus air pocket length (H_0=0.93 m).

5 INTERPRETATION OF THE TESTS AND MATHEMATICAL MODEL

The analysis of the hydraulic transients generated by venting and their comparison with similar transients in a system with an orifice suggested an interpretation of the particular features detected in the trend of p(t). In order to validate this interpretation and, at the same time, enable a reliable numerical simulation of the pressure transients, a mathematical model was set up (for convenience's sake, it is also schematised in three phases):

- **Phase I**: opening the ball valve results in a practically instantaneous increase in the (initially pressurised) air volume, as the volume of the air pocket is increased by the volume of the valve chamber (at atmospheric pressure). This causes the partial decompression of the pressurised air column, after which the release valve begins to vent smoothly. The described phenomenon is obviously more marked both as the pressurised air volume (i.e. Z_0) decreases and as the static pressure H_0 increases. Preliminary calculations carried out under the assumption that the air transformation of state is expressed by a polytropic equation with exponent n=1 have essentially confirmed the proposed interpretation. Therefore, on opening the ball valve, the initially pressurised air volume W_0 (corresponding to Z_0) increases almost instantly by the volume W_1 contained in the release valve chamber (at atmospheric pressure). Under the hypothesis of instantaneous operation, the mass balance equation furnishes:

$$\rho_0 W_0 + \rho_{atm} W_1 = \rho(W_0 + W_1) \quad (1)$$

where:

- ρ_{atm}: density of air at atmospheric pressure;
- ρ_0: density of air at initial pressure P_0 (corresponding to the set pressure);
- ρ: density of air at pressure P of the air column after partial decompression.

As W_0, W_1, ρ_{atm} and ρ_0 are known, from Eq. (1) it is possible to infer the value of ρ and, hence, the value of P from the polytropic equation:

$$\rho = \rho_0 \left(\frac{P}{P_0} \right)^{1/n} \quad (2)$$

- **Phase II**: the pipe venting phase is characterised by a rigid column motion, as already pointed by experimental investigations on pipes terminating in a simple orifice. Mathematical modelling of the transient can be achieved simply by means of the mass oscillation equations, the air continuity equation, the polytropic equation (in this phase it is more realistic to consider the exponent n nearly equal to 1.20, i.e. an intermediate transformation between isothermal and adiabatic) and the classic Wantzel and Saint Venant relation to calculate the air flow from the orifice (10), (14). In this specific case, it is obviously expected that venting is not complete and, thus, the simulation of the transient's second phase should be stopped for an air volume smaller than W_1;

- **Phase III**: as already pointed out, in this phase the transient is characterised by much higher period values and significantly lower pressure surges values than the tests with the pipe terminating in an orifice. This suggests that the automatic closing of the release valve nozzle takes place before the air in the valve chamber has been completely expelled. Therefore a small volume of air remains trapped in the valve chamber, acting as a 'buffer' in the following phase of the transient. Under this assumption, the variation in slope of the trend of p(t) identifies the instant that the nozzle is closed. The increase in pressure up to the maximum value is attributable to the compression of the residual air volume. The following pressure transient, rigid column motion, is thus not different from the one triggered by pressurising a plugged pipe with an air pocket trapped at the end (5), (9). This interpretation would also explain the deviations recorded in the trend of the transient's third phase, with particular attention to the value of ΔH_4, which are due to the way that the release valve operates: in fact, the nozzle closure may vary randomly from test to test and, consequently, the volume of air trapped in the device and compressed by the water column may also vary.

To achieve the mathematical modelling of phase III (mass oscillations in the pipe with an air cushion at the end), reference was obviously made once again to the mass oscillation and polytropic equations (9) reported below:

$$\frac{dV}{dt} = g\frac{H_0 - H}{L} - g\frac{V|V|}{K_S^2 \left(\frac{D}{4}\right)^{\frac{4}{3}}} \tag{3}$$

$$\frac{dW}{dt} = -\sigma V \tag{4}$$

$$\frac{dH^*}{dt} = -n\frac{H^*}{W}\frac{dW}{dt} \tag{5}$$

where:

- V: water column velocity;
- g: acceleration due to gravity;
- H: relative pressure;
- H^*: absolute pressure;
- L: water column length;
- D, σ: diameter and cross section of the pipe;
- K_S: Gauckler-Strickler coefficient;
- W: air volume.

Application of the mathematical model by simply setting the residual volume of air trapped in the valve chamber $W_{fin} < W_1$, enabled a satisfactory qualitative simulation of the detected pressure transients, thus confirming the proposed interpretation and, in particular, the rigid column motion.
A reliable quantitative simulation, on the other hand, presupposes the identification (obviously by successive attempts) of the actual volume of residual air W_{fin} trapped in the valve chamber when the float rises, which acts as a buffer in the transient's final phase. Figures 4 and 5 report, by way of an example, the simulations performed for $W_{fin}=0.18 \cdot W_1$ (Figure 4) and $W_{fin}=0.61 \cdot W_1$ (Figure 5), which are in good agreement with the experimental measurements up to the maximum pressure surge value (which is of greater interest from the technical standpoint). In addition, the calculations were made assuming $K_S=75\ m^{1/3}/s$ and n=1.20 and making the nozzles' outflow coefficient nearly equal to 0.75.

6 CONCLUDING REMARKS

The experimental analysis of pressure surges generated by the venting of air pockets from a pressurised pipe ending in an automatic release valve of the small-orifice type has highlighted a rigid column motion both during the venting process and after the float has risen to close the nozzle. The entrapment of a residual volume of air in the valve chamber triggers a phase of mass oscillation in the pressurised pipe with an "air buffer" trapped at the end, with fairly small pressure surge values. The mathematical model that was set up confirmed the above observations and also enabled a satisfactory simulation of the experimental transients.
The study carried out thus makes it possible to conclude that the venting of pressurised water systems under operating pressures by air valves of the small-orifice type generally does not

constitute a cause for concern, from the technical standpoint, for system managers, bearing also in mind the presumably very small volumes of air pockets to be eliminated.
Investigations still need to be conducted on the effects of generally much higher pressure surges caused by the operation of air release valves of the large-orifice type while the water system is filling. Further experiments are currently in progress in order to measure their magnitude and hence their incidence in technical terms.

REFERENCES

1. G. De Martino, M. Giugni, M. Viparelli, 1985. *La presenza dell'aria nelle condotte*, Idrotecnica, 1.
2. M.L. Albertson, J.S. Andrews, 1971. *Transients caused by air release, Control of flow in closed conduits*, ed. J. P. Tullis, Fort Collins, Colorado.
3. J.E. Funk, D.J. Wood, L.S. Reddy, D.C. Denger, 1992. *Pressure surge due to rapid expulsion of air, Unsteady Flow and Fluid Transients*, ed. Bettess & Watts, Balkema, Rotterdam.
4. D. Stephenson, 1997. *Effects of Air Valves and Pipework on Water Hammer Pressures*, Journal of Transportation Engineering, Vol. 123, No. 2, ASCE.
5. G. Benfratello, 1958. *Sulle sovrappressioni che si suscitano alla fine del riempimento delle tubazioni mobili*, L'Acqua, 5.
6. V.L. Streeter, E.B. Wylie, 1967. *Hydraulic Transients*, Mc Graw–Hill Book Company.
7. D.A. Kolp, 1968. *Water hammer generated by air release*, Master Thesis, Colorado State University, Fort Collins.
8. J.S Andrews, 1970. *Water hammer generated during pipeline filling*, Master Thesis, Colorado State University, Fort Collins.
9. C.S. Martin, 1976. *Entrapped air in pipelines*, 2nd BHRA International Conference on Pressure Surges, The City University, London, Paper F2.
10. G. De Martino, M. Giugni, M. Viparelli, 1985. *Sovrappressioni nell'efflusso da sfiati*, Quaderni dell'Accademia Pontaniana, Quaderno n. 6.
11. C.S. Martin, N.H. Lee, 2000. *Rapid expulsion of entrapped air through an orifice*, Proceedings of the 8th International Conference on Pressure Surges, Safe Design and Operation of Industrial Pipe Systems, The Hague, The Netherlands.
12. F. Zhou, F.E. Hicks, P.M. Steffler, 2002. *Transient Flow in a Rapidly Filling Horizontal Pipe Containing Trapped Air*, Journal of Hydraulic Engineering, Vol. 128, No. 6, ASCE.
13. G. De Martino, M. Giugni, M. Viparelli, 1986. *Transitori in condotte idriche causati da fuoriuscita d'aria*, Idrotecnica, 2.
14. G. De Martino, C. Gisonni, M. Giugni, M. Viparelli, 2000. *Pressure surges in water mains caused by air release*, Proceedings of the 8th International Conference on Pressure Surges, Safe Design and Operation of Industrial Pipe Systems, The Hague, The Netherlands.
15. F.J. Arregui, J. Garcia-Serra, A.C.H. Kruisbrink, E. Cabrera, V.S. Fuertes, C.V. Palau, L. Gascon, 2003. *Air valve dynamic behaviour*, PEDS 2003 - Pumps, Electromechanical Devices and Systems applied to Urban Water Management, IWA and IAHR, Valencia.

16. G. De Martino, N. Fontana, M. Giugni, 2003. *Pressure surges in water systems caused by air venting*, PEDS 2003 - Pumps, Electromechanical Devices and Systems applied to Urban Water Management, IWA and IAHR, Valencia.
17. G. De Martino, N. Fontana, M. Giugni, 2002. *Transitori conseguenti al riempimento di una condotta*, 28° Convegno di Idraulica e Costruzioni Idrauliche, Potenza, 16-19 settembre.

Notation

d: diameter of the nozzle of the air valve (or of the orifice)

D: diameter of the pipe

g: acceleration due to gravity

H: relative pressure head on the orifice

H_0 : static relative pressure head on the orifice

H^* : absolute pressure

K_s : Gauckler-Strickler coefficient

L: water column length

n: polytropic exponent

P: absolute pressure

P_0 : static absolute pressure

t: time

T: duration of transient's second phase

V: water column velocity

W: air volume

W_0 : initial air volume (corresponding to Z_0)

W_1 : volume of the air release valve chamber

W_{fin} : residual air volume entrapped in the air release valve chamber

Z_0 : length of the air pocket

ΔH_1 : initial partial decompression of the air column

ΔH_2 : maximum negative pressure variation in transient's second phase

ΔH_3 : maximum positive pressure variation in transient's second phase

ΔH_4 : maximum negative pressure variation in transient's third phase

ΔH_5 : maximum positive pressure variation in transient's third phase

ρ : density of air at pressure P

ρ_0 : density of air at static pressure

ρ_{atm} : density of air at atmospheric pressure

σ: cross section of the pipe